



## Original Article

# Life history and chromosome organization determine chemoreceptor gene expression in rattlesnakes

Michael P. Hogan<sup>1,2,\*</sup>, Matthew L. Holding<sup>1,2,3</sup>, Gunnar S. Nystrom<sup>1</sup>, Kylie C. Lawrence<sup>1</sup>, Emilie M. Broussard<sup>1</sup>, Schyler A. Ellsworth<sup>1</sup>, Andrew J. Mason<sup>4</sup>, Mark J. Margres<sup>5</sup>, H. Lisle Gibbs<sup>4</sup>, Christopher L. Parkinson<sup>6</sup>, Darin R. Rokyta<sup>1</sup>

<sup>1</sup>Department of Biological Sciences, Florida State University, Tallahassee, FL, United States

<sup>2</sup>Department of Ecology and Evolutionary Biology, University of Michigan, Ann Arbor, MI, United States

<sup>3</sup>Life Sciences Institute, University of Michigan, Ann Arbor, MI, United States

<sup>4</sup>Department of Evolution, Ecology and Organismal Biology, The Ohio State University, Columbus, OH, United States

<sup>5</sup>Department of Integrative Biology, University of South Florida, Tampa, FL, United States

<sup>6</sup>Department of Biological Sciences, Clemson University, Clemson, SC, United States

\*Corresponding author: Department of Ecology and Evolutionary Biology, University of Michigan, 1105 N. University Ave., Ann Arbor, MI 48109-1085, USA.  
Email: [mpmorgan@umich.edu](mailto:mpmorgan@umich.edu)

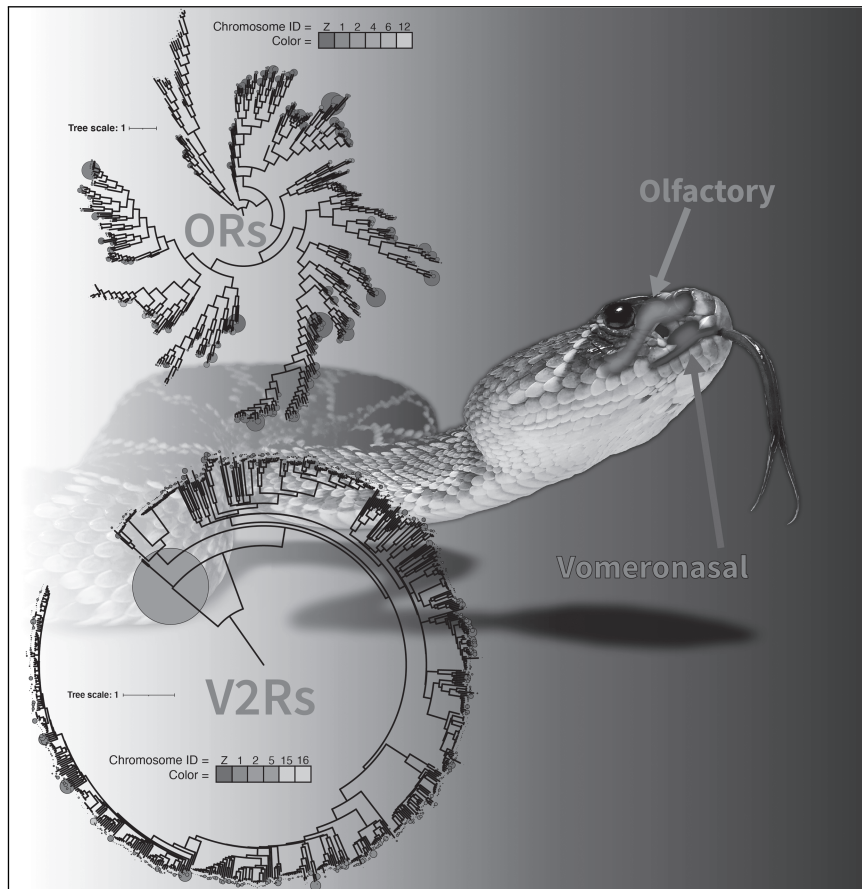
Corresponding Editor: Emma Teeling

## Abstract

Predatory species who hunt for their prey rely on a suite of integrated characters, including sensory traits that are also used for nonpredatory behaviors. Linking the evolution of sensory traits to specific selection pressures therefore requires a deep understanding of the underlying genetics and molecular mechanisms producing these complex phenotypes. However, this relationship remains poorly understood for complex sensory systems that consist of proteins encoded by large gene families. The chemosensory repertoire of rattlesnakes includes hundreds of type-2 vomeronasal receptors and olfactory receptors, representing the two largest gene families found in the genome. To investigate the biological importance of this chemoreceptor diversity, we assessed gene expression in the eastern diamondback rattlesnake (*Crotalus adamanteus*) and identified sex- and age-biased genes. We found type-2 vomeronasal receptor expression in the vomeronasal epithelium was limited to juvenile snakes, suggesting the sensory programming of this tissue may be correlated with early life development. In the olfactory epithelium, we found subtle expression biases that were more indicative of life history rather than development. We also found transcriptional evidence for dosage compensation of sex-linked genes and trait integration in the expression of transcription factors. We overlay our molecular characterizations in *Crotalus adamanteus* onto updated olfactory receptor and type-2 vomeronasal receptor phylogenies, providing a genetic road map for future research on these receptors. Finally, we investigated the deeper macroevolutionary context of the most highly expressed type-2 vomeronasal receptor gene spanning the rise of tetrapods and estimated the strength of positive selection for individual amino acid residues in the predicted protein structure. We hypothesize that this gene may have evolved as a conserved signaling subunit to ensure consistent G-protein coupled receptor functionality, potentially relaxing signaling constraints on other type-2 vomeronasal receptor paralogs and promoting ligand binding specificity.

**Keywords:** chemosensory, chromosome, gene expression, genomics, rattlesnake

## Graphical Abstract



**Keywords:** chemosensory, chromosome, gene expression, genomics, rattlesnake

## Introduction

Many species rely on the sensory perception of chemical cues for detecting and tracking resources related to fitness such as food, shelter, mates, competition, and offspring. The ability to distinguish chemical signatures is fundamentally linked to the repertoire of chemosensory receptor genes present in the genome (Niimura and Nei 2006; Hansson and Stensmyr 2011; Cohanim et al. 2018; Baldwin and Ko 2020). Many species possess hundreds of copies of these genes (Niimura 2009), which typically occur alongside large numbers of pseudogenes, indicating evolution through a birth–death process (Dong et al. 2009; Hughes et al. 2018; Nei and Rooney 2005; Niimura and Nei 2007). The proteins coded by these genes consist of G-protein coupled receptors (GPCRs) expressed in specialized sensory tissues, where they interface with certain sensory cues to trigger the sensory signaling cascade (Chess et al. 1994; Mombaerts 2004; Rosenbaum et al. 2009).

Our functional understanding of how chemosensory repertoires evolve to change sensory phenotypes is largely limited to loss-of-function scenarios following major lifestyle shifts, such as transitioning from terrestrial to marine habitats (Kishida et al. 2007; Kishida and Hikida 2010; Liu et al. 2019) or switching to a new sensory mode such as relying on echolocation in place of vision (Simoes et al. 2018). Functional

assumptions based on *in vitro* characterizations are restricted to model systems (Dong et al. 2009; de March et al. 2023) and small monomeric receptors (such as olfactory or taste receptors between 300 and 400 amino acids), which are typically one-sixth the size of a putatively functional vomeronasal receptor dimer complex. The selective pressures driving the evolution of chemoreceptor gene families can also be obscured by extreme paralogy or gene copy-number (Stranger et al. 2007; Olender et al. 2012) and intraspecific variation tied to life history such as age or sex (Rokyta et al. 2017). Parsing out the multiple levels of complexity inherent in the chemosensory gene repertoire clearly requires a deep understanding of the ecological context and the molecular landscape underlying the evolution of these traits (Khan et al. 2015).

Rattlesnakes display predatory and life-history specific chemosensory behaviors using their vomeronasal organ (Alving and Kardong 1996) and olfactory epithelial tissues lining the nasal passageway (Kardong and Berkhoudt 1999). These chemosensory behaviors include the ability to distinguish envenomated versus non-envenomated prey (Saviola et al. 2013), the detection and tracking of potential mates by male rattlesnakes from distances of up to a kilometer (Duvall et al. 1992), juveniles following adult pheromones to overwintering sites (Weldon et al. 1992), and maternal care behaviors between female rattlesnakes and her offspring

(Weldon et al. 1992). These overlaps between chemical perception and fitness present rattlesnakes as relevant study systems for understanding the biological relevance and mechanistic basis for chemoperception. Additionally, their reliance on thermal sensing (Gracheva et al. 2010) and venom (Margres et al. 2016) for predation provides an opportunity for understanding the evolutionary response of phenotypic integration and identifying genetic signatures of prey specificity (Holding et al. 2021).

The rattlesnake chemosensory repertoire includes hundreds of type-2 vomeronasal receptors (V2Rs) and olfactory receptors (ORs), representing the two largest copy-number gene families found in the genome (Hogan et al. 2021). To investigate the relative biological importance of individual chemoreceptors, we assessed gene expression from two distinct chemosensory tissues in the eastern diamondback rattlesnake (*Crotalus adamanteus*). Previous work in this system has identified venom ontogeny as profoundly influencing this predatory phenotype (Margres et al. 2015; Wray et al. 2015; Rokyta et al. 2017; Schonour et al. 2020; Hogan et al. 2024) in response to dietary shifts as the snake grows (Means 2017). In fact, ontogeny was found to explain more variance in venom expression than geography (Rokyta et al. 2017), and this major transition was later associated with the differential expression of key transcription factor regulators (TFs) and chromatin modifications (Hogan et al. 2024). Presumably, a changing diet also requires the detection of distinct chemical cues generated by different prey. To investigate the genetics underlying rattlesnake chemoperception, we sequenced mRNA isolated from two regions: The olfactory epithelial lining within the nasal passageway, and the vomeronasal epithelium (VNO) that receives cues from the forked-tongue (located rostrally on the upper palate).

Since snakes also rely on their chemosensory repertoire for behaviors such as mate detection, our sampling targeted juvenile, adult, male, and female rattlesnakes. We investigated chemoreceptor gene expression and quantified the biological importance of genes based on transcriptional biases linked to life history (Peng et al. 2022). Utilizing a telomere-resolution genome assembly for this species, we fully resolved the chromosomal organization of the chemosensory repertoire. To identify potential regulatory candidates controlling gene expression in the rattlesnake chemosensory tissues, we also investigated the expression of TF coding genes (Kawajiri et al. 2014).

Previous work on pitviper venoms reported joint roles of protein sequence variation and differential gene expression in shaping dietary adaptations (Mason et al. 2022; Schield et al. 2019; Giorgianni et al. 2020). We hypothesized that mapping the chemosensory expression patterns to other molecular characteristics would provide a similar level of improved clarity to our understanding of the chemosensory repertoire. To better understand how chemosensory gene expression relates to gene sequence variation, chromosomal organization, and protein evolution, we synthesize these molecular characterizations of rattlesnake ORs and V2Rs onto updated gene phylogenies for *C. adamanteus*. Finally, we investigated the deeper evolutionary history of the most highly expressed V2R gene, which we hypothesize evolved as a conserved signaling subunit to ensure consistent GPCR signaling from a diversity of V2R heterodimers. We compiled orthologous gene coding sequences with syntenic support from a diversity of vertebrate species, reconstructed the evolution of this V2R spanning the

rise of tetrapods, and estimated positive selection on individual residues in a three-dimensional (3D) model of the protein structure.

## Materials and methods

### Sampling and sequencing

A total of 15 *C. adamanteus* were used for chemosensory tissue RNA-seq (Supplementary Tables S1 and S1). All animals were collected in North Florida under the following scientific collecting permits: Florida USA permits LSSC-13-00004A, LSSC-13-00004B, and LSSC-13-00004C. All animal procedures were performed under active IACUC protocols at Florida State University: #0924, #1230, #1333, #1529, and #1836.

Tissue samples were dissected from chemosensory structures postmortem via the roof of the buccal cavity in the mouth. We targeted two distinct epithelial tissues representing the olfactory and the vomeronasal chemosensory pathways. We had more samples from the olfactory epithelium ( $n = 14$ ) than the vomeronasal epithelium ( $n = 9$ ) due to the latter proving more difficult to isolate consistently. Tissue samples were buffered and stored in RNA-later at  $-80^{\circ}\text{C}$  until RNA extraction. Total RNA was extracted as previously described (Rokyta et al. 2012) using the NEBNext Poly(A) mRNA Magnetic Isolation Module (New England Biolabs) and libraries were prepared for 150 nucleotide paired-end Illumina sequencing using NEBNext Ultra RNA-seq kits I and II (Supplementary Table S3). Olfactory epithelium and vomeronasal epithelium were processed separately and uniquely indexed using Multiplex Oligos from Illumina (New England Biolabs) (Rokyta et al. 2017). Libraries were visualized and assessed for size and quality using a Bioanalyzer with a high-sensitivity DNA Kit (Aligent Technologies) and amplifiable concentrations were determined using an NGS Library Quantification Kit (KAPA Biosystems). Individual libraries were pooled and sequenced with 150 nucleotide paired-end reads at the Florida State University College of Medicine Translational Science Laboratory on an Illumina HiSeq 2000. Read quantity and quality were assessed with FastQC version 0.11.9. We performed adapter and quality trimming using Trim Galore! version 0.6.6 with settings `--length 50 -q 10 --stringency 1-e 0.1`. Reads were aligned to the reference genome (Hogan et al. 2024) using hisat2 version 2.2.1 (Kim et al. 2019) with parameters `--no-unal --max-intronlen 25000 --dta` and sorted using samtools (Li et al. 2009) version 1.12. Read counts, trimming and aligning percentages, and sequencing details for all rattlesnake chemosensory transcriptomes are included in Supplementary Table S3.

We utilized the original gene annotations that were published previously alongside the initial release of the reference genome by Hogan et al. (2024). In an effort to promote methodological transparency, we reiterate the full gene annotation protocol in Supplementary SI document to accompany this study. Briefly, chemosensory genes were initially predicted using previous meticulous characterizations in this species (Hogan et al. 2021). This rough-pass resulted in 1,037 potential OR genes and 998 potential V2R genes. These were then quality-filtered based on their translated protein sequences. We assigned putatively functional ORs and V2Rs based on the completeness of conserved protein domains, which a functional G-protein coupled receptor (GPCR) requires (e.g. intact 7-transmembrane region). The final chemoreceptor

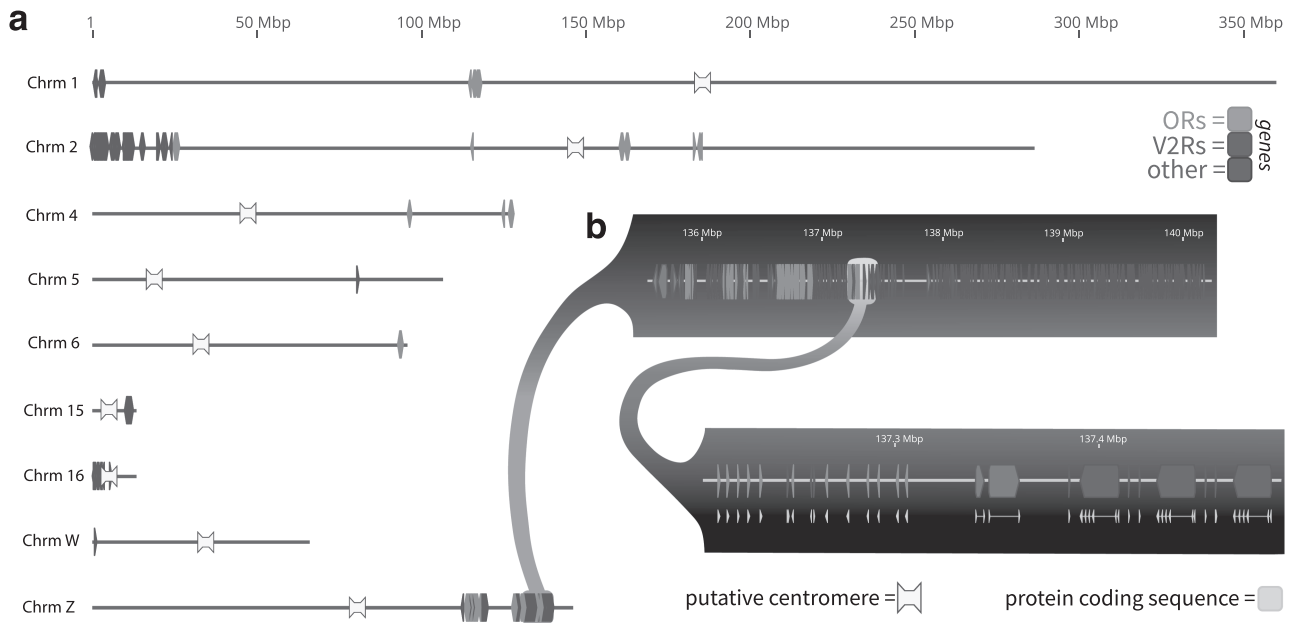


**Fig. 1.** Chromosomal locations of all putative OR and V2R genes in *C. adamanteus*, and a zoomed in tandem repeat gene cluster on chromosome Z. (a) Chemosensory genomic architecture is shown with OR genes colored orange and V2Rs colored purple. Putative centromere locations are also visualized in white. (b) The zoomed-in region illustrates the genomic breakdown of a large gene array present on chromosome Z, including additional non-chemosensory genes shown in gray and coding sequence spanning exonic structures underneath in yellow. ORs typically contain their entire coding sequence within a single exon, while V2Rs typically span across 6 exons.

gene counts after filtering included 493 putatively functional ORs and 687 putatively functional V2Rs (Fig. 1). For the sake of clarity, this study only investigates full-length genes coding for putatively functional receptors and ignores pseudogenes and/or orphaned exons. Additional context is provided in the Supplemental SI document.

Since assigning sex to juvenile snakes morphologically is not always reliable, we confirmed sex using *W* chromosome gene expression profiles (Supplementary Fig. S2a), where expression was only expected in females. This procedure corrected our original sex assignment for one of the juvenile snakes (ID = DRR0139). One transcriptome (ID = DRR0044) was previously submitted by Hogan et al. (2021) as a “combined olfactory and vomeronasal” transcriptome. To determine if the vomeronasal signal was strong enough to justify including it as our only male juvenile sample, we compared all samples using PCA plots (Supplementary Fig. S1) and confirmed that this sample grouped more with the other juvenile vomeronasal samples than with the olfactory or adult tissues. On the basis of this confirmation, we included this sample with our vomeronasal sampling for downstream analyses.

### Differential expression analyses

Using the previously quality-checked, trimmed, and aligned RNA-seq datasets, we compared gene expression between male and female rattlesnakes and adult and juvenile rattlesnakes using DESeq2 v1.32.0 (Love et al. 2014) in R. DESeq2 accounts for overdispersion (variance > mean) by using a negative binomial distribution to model normalized RNA-seq counts for each gene. Read counts were initially calculated with HTSeq-count v0.13.5 (Putri et al. 2022) using gene coding sequence annotations as the reference. To minimize any confounding effects due to the non-target bias per test (i.e. sex for age and age for sex), we included these as

parameters in our DESeq2 DE model design. We assigned expression bias using  $\log_2$ -fold change > 1 and FDR < 0.05 as our set threshold across all expression analyses. This threshold accounts for inflated false positive rates (i.e. the multiple testing problem) since FDR values reported by DESeq2 represent adjusted *P*-values after correcting for multiple testing and low expression using the Benjamini and Hochberg method (Benjamini and Hochberg 1995). By setting the FDR cutoff to <0.05, we assume that the proportion of false positives amongst our differentially expressed genes is 5%. We considered this combined with the secondary  $\log_2$ -fold change criteria as a conservative approach. Differentially expressed (DE) genes were classified as adult-, juvenile-, male-, or female-biased depending on the  $\log_2$ -fold change direction (i.e. negative vs. positive). To contextualize our significant chemosensory gene findings relative to all other expressed genes, we visualized the full differential expression test results as volcano plots using the R package EnhancedVolcano v1.10.0 (Fig. 2). Life history biased gene expression of ORs, V2Rs, and TFs was visualized in greater detail as heatmaps using the R package pheatmap v1.0.12 (Fig. 3 and Supplementary Figs S2 and S3). All heat plots depict expression differences with cell colors based on regularized log (rlog) count differences per gene (i.e. row). Full results from the DESeq2 expression tests are available in Supplementary File 2.

### Phylogenetics and selection analyses

We generated updated OR and V2R gene phylogenies for *C. adamanteus* and mapped chromosome assignments based on a highly contiguous chromosome resolution genome assembly for this species (Hogan et al. 2024). These phylogenies fully capture the sequence variation across paralogs in a single species (Figs 4 and 5). We translation-aligned OR and

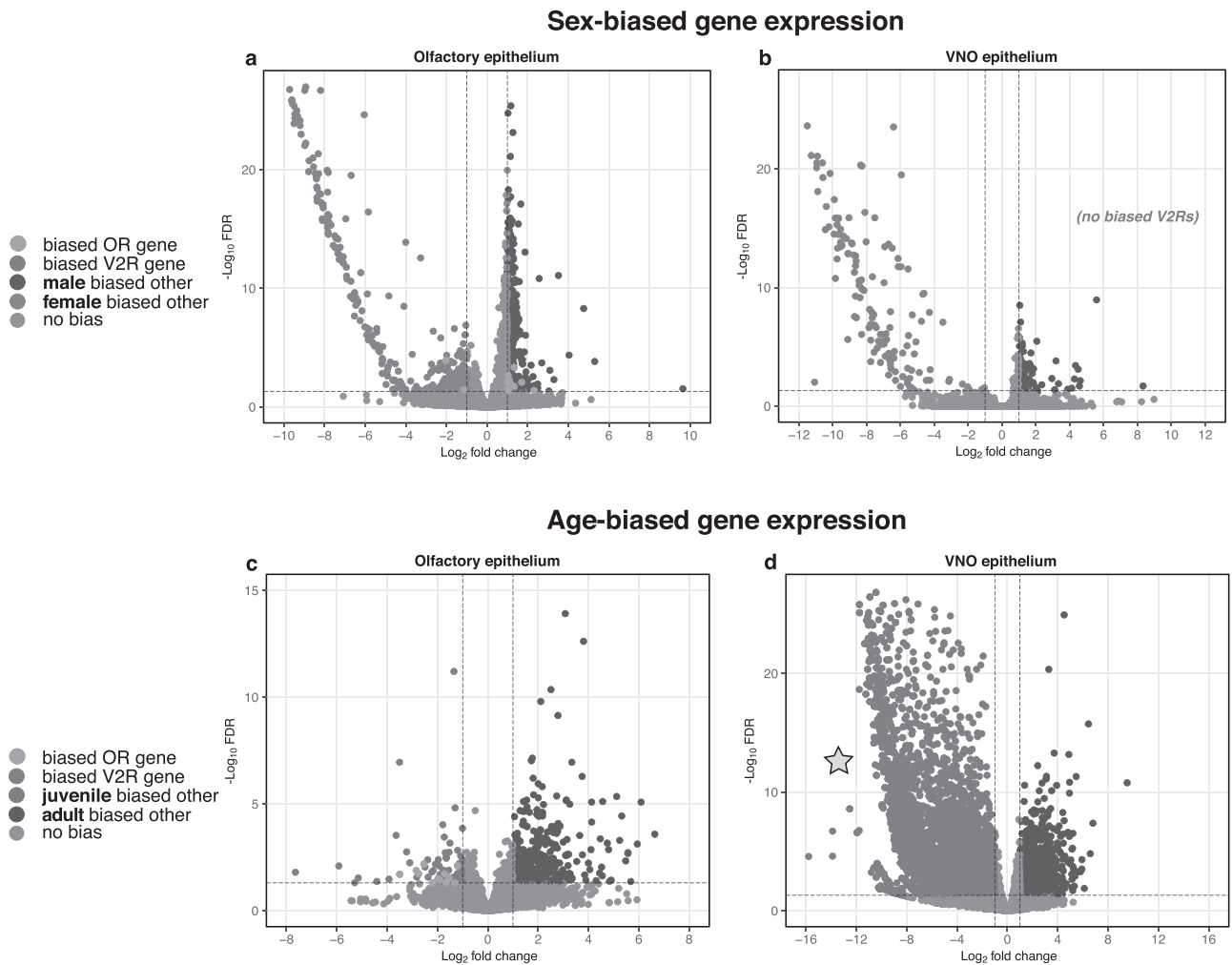


**Fig. 2.** Chemosensory tissue volcano plots illustrate genome-wide expression across all genes and biased expression between age and sex groups. The expression bias significance cutoff used for all analyses was  $\log_2$ -fold change  $> 1$  and FDR  $< 0.05$  (a) From the olfactory epithelium, we identified sex-biased genes including male- and female-biased ORs. (b) From the vomeronasal epithelium, we identified sex-biased genes but no sex-biased V2Rs. (c) From the olfactory epithelium, we identified age-biased genes but only juvenile-biased ORs. (d) From the vomeronasal epithelium, we identified an unexpected and overwhelming expression bias towards juvenile rattlesnakes, with a yellow star highlighting a probable developmental transition. Far fewer genes and no V2Rs were biased towards adult expression.

V2R nucleotide coding sequence codons using Clustal Omega v1.2.3 (Sievers et al. 2011). All codons per alignment were assigned as either extracellular, intracellular, or transmembrane based on matches to the Conserved Domain Database (CDD; Marchler-Bauer et al. 2014; Lu et al. 2019). Resulting codon alignments were utilized for downstream phylogenetic reconstructions, selection analyses, and protein inferences. Maximum likelihood trees were built for each alignment using IQ-TREE v2.2.0 (Nguyen et al. 2014; Chernomor et al. 2016; Kalyaanamoorthy et al. 2017; Hoang et al. 2017). Input alignments were specified as codon data using the `-st CODON` option, and the best substitution models were chosen automatically using ModelFinder (Kalyaanamoorthy et al. 2017). Branch support was assessed using ultrafast bootstrap approximations and single branch SH-like approximate likelihood ratio tests using the `-B` and `-a1rt` commands with 1000 replicates each (Hoang et al. 2017; Guindon et al. 2010). Tree figures were generated using iTOL via their online server (Letunic and Bork 2019).

Consensus trees and codon alignments were consolidated into nexus files (Supplementary File 3) and tested for directional selection within the HyPhy suite v2.5.8 (Pond et al. 2019). Generally, the statistical approaches implemented via HyPhy estimate nonsynonymous substitution rates and synonymous substitution rates to generate a ratio (i.e.  $dN/dS$ ), which provides information about the evolution of each codon. Estimates of pervasive selection assume a constant  $dN/dS$  for a single codon site across the entire phylogeny, and therefore summarize overall selection per site while ignoring differences between genes. We tested sites for pervasive selection using FEL v2.1 (Pond and Frost 2005) and episodic selection using MEME v2.1.2 (Murrell et al. 2012). From MEME, the per-branch selection strength is reported as an Estimated Bayes Factor (EBF) value for each site, and we followed HyPhy's suggested EBF  $> 100$  cutoff for our reporting and visualizations.

To investigate whether selected sites were correlated with structural regions, we ran proportional  $z$ -tests comparing

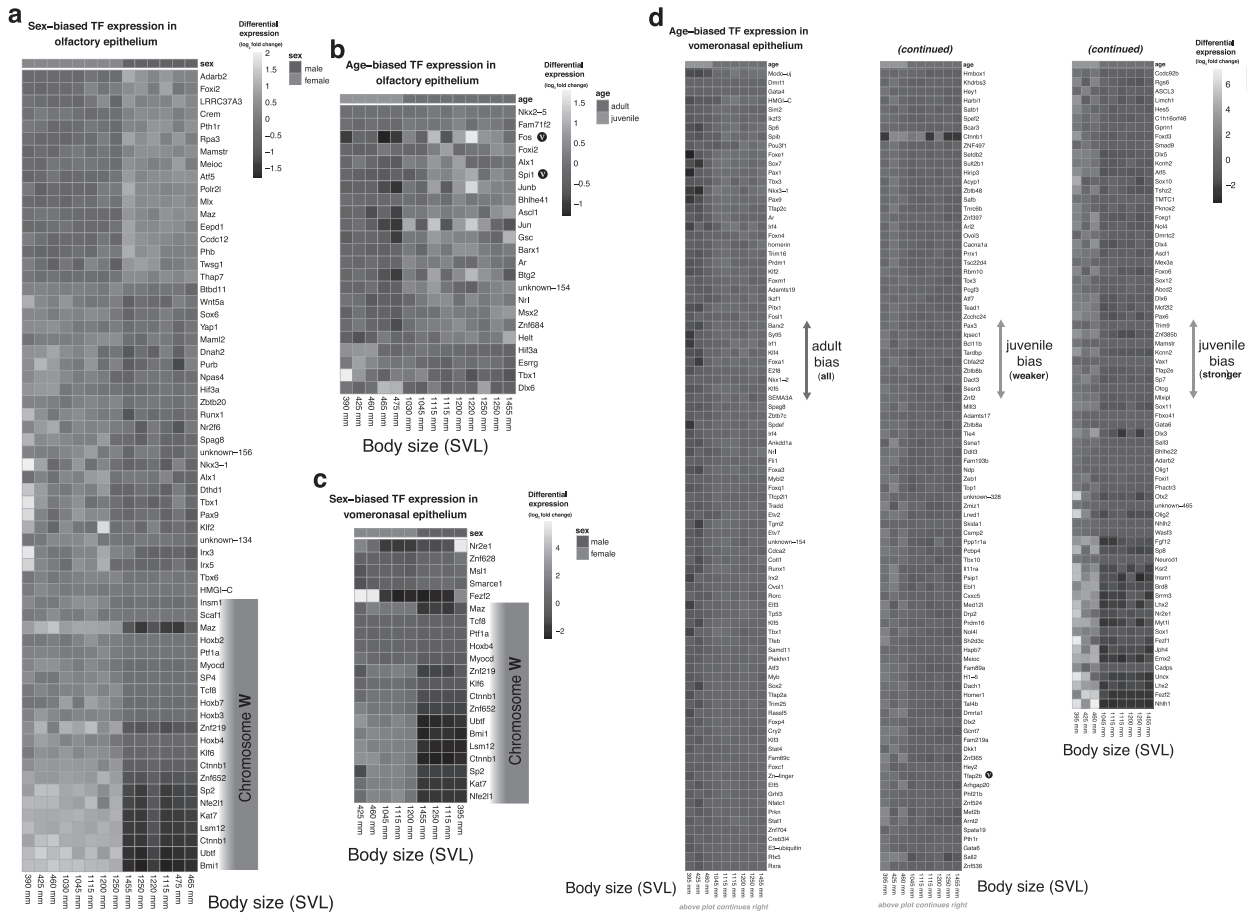


**Fig. 3.** Life-history biased TF gene expression in rattlesnake chemosensory tissues. (a) Sex-biased TF expression in olfactory epithelium. Female-biased TFs are dominated by chromosome W genes (marked with a green box). (b) Adult expression bias in TFs predicts negative regulation of juvenile-biased ORs (Supplementary Fig. S3b). Fos and Sp1 are also adult-biased in venom glands (marked with yellow “V” in black circle). (c) Sex-biased TFs in vomeronasal epithelium. Female-biased TFs occur on chromosome W, mirroring the olfactory epithelium. (d) Heatplot of age-biased vomeronasal TFs (split up for space). The overwhelming early-life development signal seen in V2Rs also manifests in TFs. The most juvenile-biased TFs (i.e. bottom third of rightmost plot) all appear to have regulatory functions consistent with sensory development. Tfpap2b is also juvenile-biased in venom glands (marked with yellow “V” in black circle).

selected sites between extracellular, intracellular, and transmembrane regions. Proportions were based on the number of selected sites out of the total sites assigned to each region of the receptor. We tested this using the FEL and MEME default selection cutoff of 0.05 for significance. With FEL, we tested if the proportion of positively selected sites was significantly higher or lower for extracellular regions vs. intracellular regions, extracellular regions vs. transmembrane regions, and intracellular regions vs. transmembrane regions. This analysis was repeated for the proportion of negatively selected sites ( $P < 0.05$ ). With MEME, we tested if the proportion of episodically diversifying sites was significantly higher or lower for extracellular regions vs. intracellular regions, extracellular regions vs. transmembrane regions, and intracellular regions vs. transmembrane regions. This was repeated for branch codons ( $P < 0.05$ ). These results are shown in Table 1. All selection test results, protein domain statistical tests, and all sites reported by MEME with an EBF > 100 are included in Supplementary File 4.

We implemented a similar breakdown analysis to investigate the selection results we generated from MEME based on chromosome composition. Specifically, we predicted

chromosome ancestral states for all branches across the OR and V2R gene tree using ape v5.8 in R (Paradis and Schliep 2019). We then mapped all positively selected codon branch sites from MEME (EBF > 100) to their corresponding predicted chromosome state, and finally implemented a series of z-tests comparing proportions of selected sites per total available sites on each chromosome, giving us a clear breakdown of which chromosomes likely have positive selection hotspots relative to the other chromosomes. Similar to our protein domain selection evaluation tests, we again favored a proportional framework that appropriately accounts for different chromosomes having different numbers of genes and therefore different numbers of sites for selection to act upon. The ancestral state reconstruction results and chromosomal selection composition stats are included in Supplementary File 4.

### Multi-species analysis

We investigated the macroevolutionary context of a single V2R gene (orthologous to gene ID = V2R-426-chrm5\_gene11962), which represents the only V2R gene occurring on chromosome 5 and is the most highly expressed

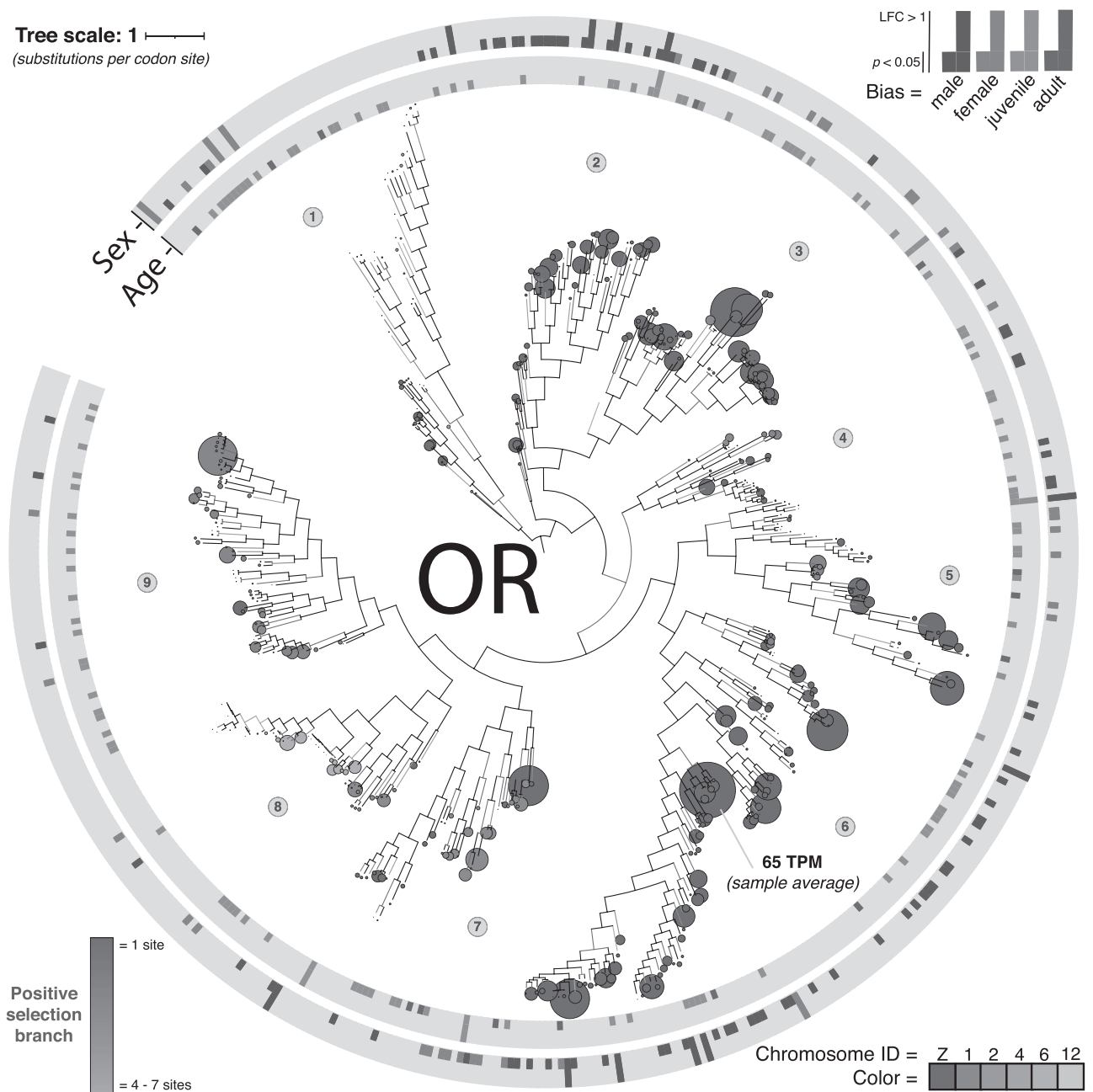


**Fig. 4.** OR gene tree for *C. adamanteus* overlaid with expression results and chromosome placement. The phylogeny is a maximum likelihood gene tree of codon-aligned coding sequences rooted at the midpoint. Branch lengths represent number of nucleotide substitutions per codon. Branches are shaded green based on signatures of episodic positive selection detected in extracellular sites (MEME analysis; empirical Bayes factor > 100): black = no selection, dark green = fewer sites detected per branch, and light green = more sites detected per branch. Circles at tree tips are proportionally scaled based on average expression (TPM) for all 19 samples and are colored by chromosome. Expression bias results surround the tree, showing genes we called significant with a long rectangle and genes with FDR < 0.05 but  $\log_2$ -fold change < 1 with a short rectangle. Numbers in light-yellow mark clades discussed in the text.

V2R gene (7.2% of all V2R expression) in *C. adamanteus*. We compiled gene coding sequences after confirming syntenic support from 19 vertebrate species including 10 snakes, 5 lizards, 1 turtle, 1 frog, and 2 fish (Supplementary Table S4). Syntenic support was confirmed based on the sequence identity of conserved exons for the target V2R, downstream flanking genes *GMPS* and *SLC33A1*, and upstream flanking genes *KCNAB1* and *SSR3* (Fig. 6c). Genomes that were missing the conserved

V2R genomic region were not explored in this study; however, several of these were of reasonable quality and represented key Tetrapod lineages worth mentioning. These included hag-fish, lamprey, shark, lungfish, ray-finned fish, crocodile, bird, tuatara, human, and rodent genomes (NR database searches completed April 2023). For these major clade representatives, the missing genomic region may reflect biological reality (e.g. a deletion event) or some technical artifact. We were also unable

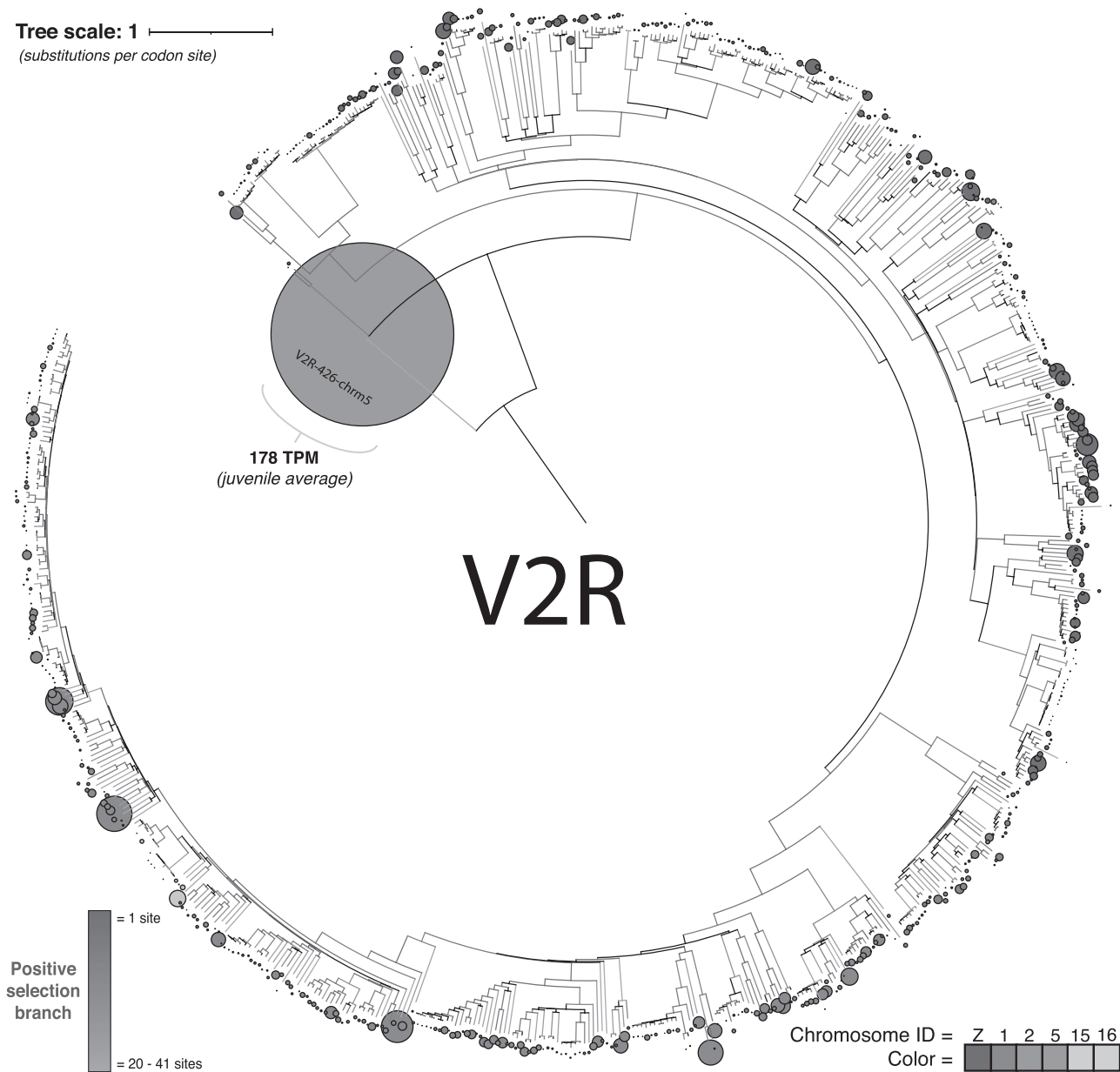


**Fig. 5.** V2R gene tree for *C. adamanteus* overlaid with juvenile expression and chromosome placement. Tree formatting including branch and circle colors mirror the OR tree from Fig. 4. Circle size depict average TPM including the 3 juvenile rattlesnake vomeronasal epithelium samples. We determined gene V2R-426-chrm5 was responsible for 7.2% of the total V2R expression, had 26 positively selected codons (EBF > 100) at the tree midpoint, and was the only V2R gene occurring on chromosome 5, leading us to investigate it further in other species.

to establish gene synteny from a representative Scolecophidian snake (i.e. blind snake) since all available genomes were below the resolution needed for syntenic confirmation.

Using the 19 species V2R coding sequences, we mirrored the alignment and tree-building steps described earlier for the two single-species paralog trees. We also performed MEME (Murrell et al. 2012) to evaluate periods of elevated positive selection. The resulting 19 species maximum likelihood phylogeny captures the evolution of this V2R in vertebrates (Fig. 6a). To better interpret how selection influenced the receptor protein structure, we modeled a reference heterodimer structure using SWISSMODEL ExPasy via their online server (completed February, 2023; Waterhouse et al. 2018; Guex et al.

2009; Bertoni et al. 2017). Structure for this model was predicted based on similarity to heterodimeric metabotropic glutamate receptors (Wu et al. 2014; Du et al. 2021). Episodic selection was mapped onto this structure using EBF > 100 from the MEME selection test. We then interpreted structural transitions predicted at exposed extracellular residues experiencing strong signals of episodic positive selection, highlighting two noteworthy residues. The first is predicted to have influenced changes to the dimer interface between amphibians and in a reptile common ancestor and represents the only positively selected extracellular dimer interface residue on the tree. The second is predicted to have influenced changes to the extracellular scent binding pocket between lizards and snakes,

**Table 1.** Summary of codon based proportional z-tests comparing the total extracellular, intracellular, and transmembrane sites experiencing selection for ORs and V2Rs. Significant results are shown in bold ( $P < 0.05$ ), and the z direction (positive versus negative) indicates which of the two domains are biased for each comparison (shown above).

OR proportional z-tests	Proportion of extracellular with selection	Proportion of intracellular with selection	Proportion of transmembrane with selection	Extracellular (+z) vs intracellular (-z)		Extracellular (+z) vs transmembrane (-z)		Intracellular (+z) vs transmembrane (-z)	
				P	z	P	z	P	z
FEL pervasive negative selection	0.497	0.385	0.947	0.0656	1.84	<0.00001	-9.52	<0.00001	-10.88
FEL pervasive positive selection	0.00662	0.00820	0.00	0.879	-0.152	0.261	1.12	0.211	1.25
MEME episodic positive	0.0331	0.0574	0.163	0.331	-0.972	<b>0.000104</b>	-3.88	<b>0.00531</b>	-2.79
MEME episodic positive + branch	0.00	0.00	0.000900	0.225	1.21	<0.00001	-6.91	<0.00001	-7.29

V2R proportional z-tests	Proportion of extracellular with selection	Proportion of intracellular with selection	Proportion of transmembrane with selection	Extracellular (+z) vs intracellular (-z)		Extracellular (+z) vs transmembrane (-z)		Intracellular (+z) vs transmembrane (-z)	
				P	z	P	z	P	z
FEL pervasive negative selection	0.528	0.639	0.862	<b>0.0378</b>	-2.08	<0.00001	-8.00	<b>0.0000243</b>	-4.22
FEL pervasive positive selection	0.0176	0.0206	0.0120	0.835	-0.209	0.601	0.523	0.579	0.554
MEME episodic positive	0.317	0.165	0.156	<b>0.00203</b>	3.09	<b>0.00</b>	4.18	0.843	0.198
MEME episodic positive + branch	0.00233	0.000551	0.00	<0.00001	13.23	<0.00001	12.87	<b>0.0000191</b>	-4.28

and represents the highest ancestral extracellular EBF value detected from the tree (Fig. 6b; Supplementary File 4).

## Results

### Distinct gene expression profiles for olfactory and vomeronasal tissues

We assessed gene expression across the complete chemosensory gene repertoire (Fig. 1) in the eastern diamondback rattlesnake (*C. adamanteus*) and linked expression variation to specific age class (adult vs. juvenile) and sex (female vs. male) for individual chemoreceptors. V2R expression in the vomeronasal epithelium was almost entirely limited to the juvenile snakes (Fig. 2d and Supplementary Fig. S2b), suggesting sensory programming of the VNO probably coordinates with early development of the vomeronasal structures, forked-tongue, and associated chemosensory behaviors. Our limited juvenile vomeronasal sampling ( $n = 3$ ) prevented us from identifying any sex-biased V2Rs. We did not observe a similar large-scale developmental shift in the olfactory epithelium, but instead found subtle expression biases which we considered more indicative of life history. We detected 23 differentially expressed ORs out of 481 total OR genes, including 10 which were biased towards males, 2 which were biased towards females, and 12 which were biased towards juveniles. Of these, we found one Z-chromosome OR gene with overlapping biases towards males and juveniles, suggesting this receptor could be uniquely advantageous to male juveniles.

We also evaluated TF gene expression in chemosensory tissues and found sex- and age-biased genes. General TF expression patterns were consistent with chemoreceptor expression in each chemosensory tissue. The vomeronasal epithelium was overwhelmed by numerous age-biased genes, including 111 juvenile-biased TFs. Interestingly, the top juvenile-biased vomeronasal TFs (based on  $\log_2$ -fold change) all appear to perform functions regulating early life development of sensory tissues. These TFs include *Nhlh1*, *Nhlh2*, *Fezf1*, *Fezf2*, *Emx2*, *Lhx2*, *Sox1*, *Jph4*, *Fgf12*, and *Neurod1* (functions based on UniProt searches performed February 2023; UniProt Consortium 2015). We checked the NDEX database

(Shannon et al. 2003) for biological pathways overlapping with the juvenile signal and found neural crest differentiation (pathway ID = WP2064) to be the closest match (searched February 2023). We considered this to be confirmation that the extreme juvenile bias is actually an early life developmental signal. We did not explore this further, but a thorough gene-by-gene investigation of our biased TFs could help establish a deeper developmental context for the early-life sensory programming of the vomeronasal system in rattlesnakes.

From the olfactory epithelium, we found TF expression biases tied to life history, including 64 sex-biased and 23 age-biased TF-coding genes. Nineteen of the age-biased TFs were biased towards adults and four were towards juveniles, which points at negative regulation of the multiple juvenile-biased ORs. Our TF expression tests resulted in two unexpected key findings. First, we found female-biased TF expression is dominated by W chromosome genes in both the olfactory ( $n = 22$ ) and the vomeronasal epithelium ( $n = 16$ ). This pattern shows transcriptional evidence for a regulatory mechanism originating from a snake sex chromosome, where female-specific transcription factors may be enhancing female-biased gene expression and/or repressing female expression of male-biased genes. Second, two TFs associated with the AP-1 activation complex, *Fos* and *Spi1*, have adult-biased expression both in venom glands (Hogan et al. 2024) and the olfactory epithelium. This pattern provides transcriptional evidence for regulatory integration, where the AP-1 activation complex coordinates ontogenetic transitions in sensory perception and venom. We also found a shared juvenile-bias for *Tfap2b* between the vomeronasal tissue and venom glands. Although less compelling, this pattern supports AP-2 activation complex to be more important in juveniles.

### Gene sequence, chromosome, and life-history elucidate the extreme genetic complexity of rattlesnake ORs and V2Rs

Our updated OR and V2R phylogenetic representations (Hogan et al. 2021) for *C. adamanteus* greatly reduce dimensionality to our genetic understanding of rattlesnake

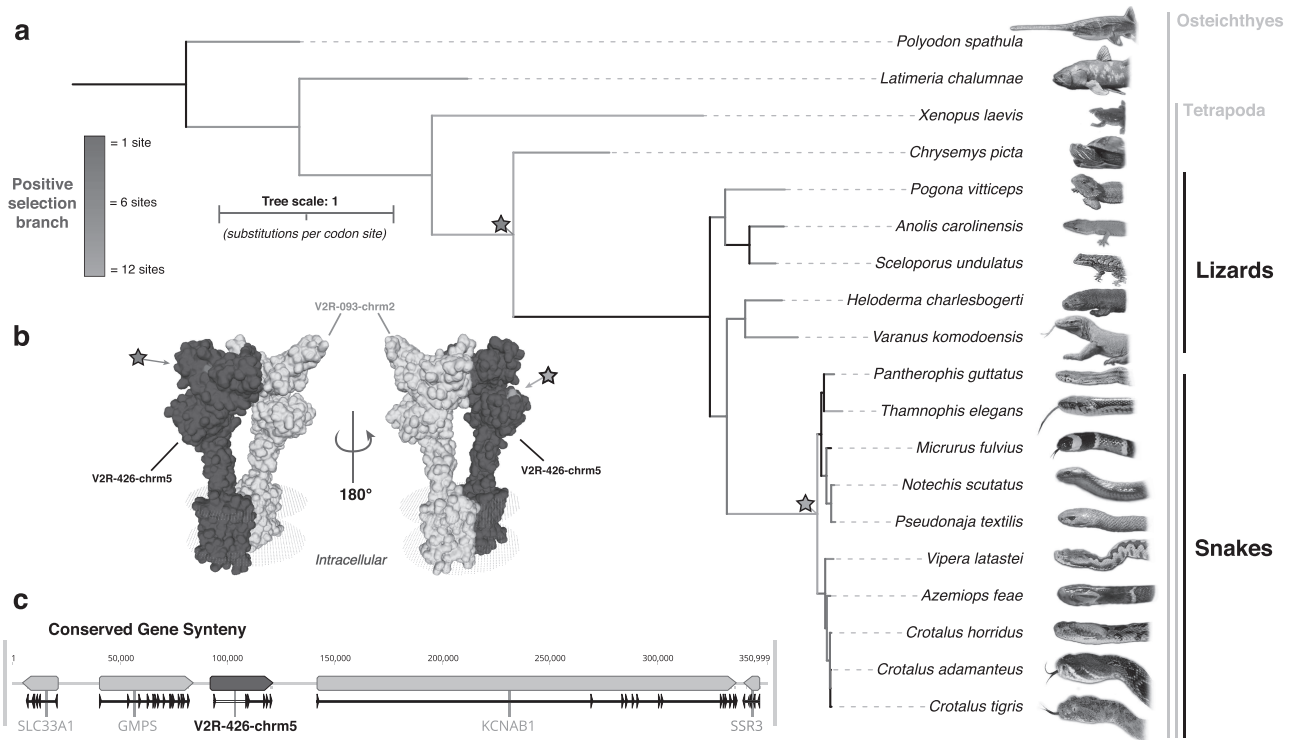


**Fig. 6.** Evolution of a V2R ortholog reconstructed from 19 vertebrate species revealing an ancient origin tracing back to bony fish. (a) Maximum likelihood phylogeny of putative V2R-426-chrm5 orthologs via codon alignment (same as Figs 4 and 5). Branches are shaded green based on signatures of episodic positive selection detected in extracellular sites (MEME analysis; empirical Bayes factor (EBF) > 100): dark green distinguishes fewer sites detected per branch and light green distinguishes more sites detected per branch. Two stars mark periods of strong transient evolution at two distinguished protein residues (details below). (b) 3D protein structure of a membrane-bound V2R heterodimer modeled for *C. adamanteus* V2R-426-chrm5 (black) and V2R-093-chrm2 (white) via SWISSMODEL Expsy (Guex et al. 2009; Bertoni et al. 2017). Structure was predicted based on homology to glutamate receptors (Wu et al. 2014; Du et al. 2021). The stars reflect 2 major sensory transitions during tetrapod VNO evolution: (1) fuchsia marks residue 86 changing part of the extracellular dimer interface (EBF = 269.2) during the rise of an ancestral reptile (i.e. turtle-lizard ancestor) from amphibians; (2) green marks residue 287 changing the structure of the ligand binding pocket (EBF = 139,687) during the rise of snakes from a lizard ancestor. (c) Highly conserved gene synteny for this single-copy V2R enabled confident ortholog identification from all 19 representative genomes including several fragmented assemblies (details in Supplementary Table S4). Image of *V. komodoensis* courtesy of Daniel Dashevsky.

chemoperception, resulting in gene subsets that are organized by molecular characterizations and phylogenetic signals. For the OR gene tree, we interpreted the molecular patterns of nine sub-clades (numbered in yellow in Fig. 4) based on relative average gene expression, life history bias, chromosomal distribution, and extracellular episodic positive selection: clade 1 has low-expression female-biased Z chromosome ORs and not expressed but diversifying autosomal ORs (11 o'clock in Fig. 4); clade 2 has medium-expression male-biased Z chromosome ORs (12 o'clock in Fig. 4); clade 3 has high-expression Z chromosome ORs and a potential translocation or duplication to chromosome 1 from Z (1 o'clock); clades 4 and 5 have medium-expression primarily non-biased Z and autosomal ORs (3 o'clock); clade 6 has high-expression Z chromosome ORs and sex-biased ORs (6 o'clock); clade 7 has high-expression Z chromosome ORs and medium-expression autosomal ORs with a weak but consistent female bias (7 o'clock); clade 8 has medium-expression non-biased autosomal ORs including all from chromosome 6 and low-expression diversifying ORs (8 o'clock); and clade 9 has medium-expression autosomal ORs with a weak but consistent juvenile bias.

For the V2R gene tree (Fig. 5), we identified a single gene (ID = V2R-426-chrm5\_gene11962) which is the only

chromosome 5 V2R and is responsible for 7.2% of all V2R expression. Top BLASTP hits suggest this is a type-1-like V2R (Sayers et al. 2022). Although the overwhelming developmental transition in the VNO prevented life-history assessment of the gene tree sub-clades, we still identified clear chromosome-based organization: all Z chromosome V2Rs appear together on the clades directly following V2R-426-chrm5 (11 o'clock to 3 o'clock in Fig. 5); all autosomal V2Rs (except for chromosome 5) appear together on a large clade comprised of many smaller clades further organized by specific autosomes (e.g. sub-clade with chromosome 15 and 16 V2Rs; colored yellow in Fig. 5). Among the autosomal V2Rs, we find lineages in the phylogeny with long branches extending from sub-clades experiencing positive selection in extracellular regions (Fig. 5). These rapidly evolving branches may be currently undergoing adaptive evolution, potentially for prey detection, suggesting the chemoreceptor repertoire is highly dynamic in both number of paralogs and sequence.

The updated gene phylogenies and codon alignments were tested for directional selection (i.e.  $dN/dS$ ) within the HyPhy suite v2.5.8 (Pond et al. 2019). We tested for pervasive selection using FEL v2.1 (Pond and Frost 2005) using a selection cutoff of 0.05 for significance. With FEL, we detected positive selection at two residues for ORs and 19 for V2Rs.

We detected pervasive purifying selection at 302 residues for ORs and 655 for V2Rs. We also tested for the signature of episodic evolution in chemoreceptor coding sequences, revealing discrete periods of positive selection on both phylogenies (Murrell et al. 2012). Unlike the pervasive tests, the episodic analysis accounts for selection differences between individual genes and branches for each codon site, which we called “branch-codons” (total branch-codons = total codon sites  $\times$  total branches). We detected episodic selection at 43 residues and 231 branch-codons in ORs and 296 residues and 2,841 branch-codons in V2Rs. These branch-based analyses allowed for more precise interpretations of selection based on individual mutation events during the diversification of these gene families.

We next ran proportion  $z$ -tests to evaluate whether the proportion of sites experiencing selection were significantly higher or lower between receptor domain regions. Our results update prior comparisons (Hogan et al. 2021) with more complete chemoreceptor gene recovery and additional consideration of transmembrane evolution in our protein domain comparisons. Results from these tests (Table 1) revealed OR transmembrane helices experienced more directional selection (i.e. positive and negative) compared to the extracellular and intracellular domains. These selection patterns suggest transmembrane interactions between ORs and other membrane-bound proteins or molecules likely played an important role in shaping the current OR diversity in *C. adamanteus*. Pervasive purifying selection in the transmembrane helices of ORs was much stronger than transient diversifying selection according to  $z$ -scores. The V2R extracellular domain experienced the most episodic diversifying selection and the least pervasive purifying selection, making it the fastest evolving region for V2Rs. This is consistent with prior reports (Hogan et al. 2021) and explains the apparent abundance of positively selected branches (colored green) on the V2R phylogeny (Fig. 5). Pervasive purifying selection was highest in the transmembrane helices of V2Rs. Based on the significantly higher pervasive negative selection detected from both OR and V2R transmembrane regions, we update prior assumptions that the cytoplasmic intracellular regions are the most conserved regions of these receptors (Hogan et al. 2021).

The selection results we generated from MEME were also evaluated for chromosome composition, which suggested certain chromosomes are probable hotspots for selection relative to the other chromosomes where these genes occur. For the ORs, we found that chromosome 4 in particular stands out from the others for having the highest supported positive selection hotspot and for having a proportional  $z$ -score that is considerably higher (+6.3) than the next highest seen in chromosome 2, while chromosome 1 has the lowest support (Supplementary Figs S4a and S5a). For the V2Rs, we found that chromosome 2 has the highest supported positive selection hotspot, while chromosome Z stands out from the others for having the least supported with a proportional  $z$ -score considerably lower (−7.5) than the next lowest seen in chromosome 16 (Supplementary Figs S4b and S5b).

### Ancient origins of one V2R indicates protein change during major sensory transitions

We investigated the macroevolutionary context of a single V2R (ID = V2R-426-chrm5\_gene11962) representing the only gene of this family occurring on chromosome 5. This particular gene is also the most highly expressed V2R (7.2% of all

V2R expression in *C. adamanteus*). To better understand the deep evolutionary history of this gene, we compared orthologous gene coding sequences with syntenic support for 19 vertebrate species, constructed a phylogeny of this V2R spanning the rise of tetrapods, and projected positive selection onto a 3D model of the protein structure (sequences accessed from NR database February 2023). Because the genomic locus containing this gene was highly conserved (Fig. 6) and distinct (i.e. single-copy), we confirmed gene synteny for all 19 species including several highly fragmented assemblies (Supplementary Table S4). The resulting 19-species maximum likelihood phylogeny rooted on the paddlefish (*Polyodon spathula*) maps the deep evolution of this V2R back to an early osteichthyan ancestor (Fig. 6a). Our protein structure modeling predicted this particular V2R shares structural homology with metabotropic glutamate receptors, which are known to form heterodimers (Wu et al. 2014; Du et al. 2021). We interpreted structural transitions predicted at two important extracellular residues experiencing strong signals of episodic positive selection. First, residue 86 is the only positively selected extracellular site (EBF = 269.2) on the tree overlapping into the dimer interface and occurred during the rise of an ancestral reptile (i.e. a turtle-lizard ancestor) from an amphibian ancestor. Based on this phylogenetic placement, we predict an important mutation which changed the dimer interface likely coincided with chemosensory phenotypes transitioning from aquatic to terrestrial perception (e.g. water versus air). Second, residue 287 is proximal to the extracellular ligand binding pocket with the highest extracellular positive selection (EBF = 139,687) detected from an internal branch on the tree, and coincided with the rise of snakes from a lizard ancestor. Due to the strength of this signal and the deep rooting of the phylogeny, we predict a beneficial mutation occurred at this residue that greatly enhanced vomeronasal acuity in the snake ancestor. Based on these findings, we hypothesize that this gene may have evolved as a conserved signaling subunit to ensure consistent G-protein coupled receptor (GPCR) signaling, perhaps from a diversity of V2R heterodimers.

### Discussion

Several studies have begun dissecting the complexities of snake chemosensory gene expression in relation to habitat, particularly regarding aquatic adaptations. Reduced numbers of OR paralogs were found to be expressed in sea snakes (Kishida et al. 2019), consistent with the assumption that ORs are more involved in detecting airborne cues. A recent study by Peng et al. (2022) compared chemosensory gene expression between aquatic and non-aquatic snakes and found higher expression of V2Rs in aquatic snakes, which is consistent with the assumption that V2Rs preferentially bind to water-soluble odor molecules. This same study also reported significant contributions of transcription factors, including several that we also reported (e.g. Lhx2, Insm1, and Foxg1). Our original motivation for investigating snake chemosensory systems aligned with studies like these, targeting sensory trait evolution in the context of trophic ecology. However, we determined capturing life history influence from a single species was a necessary first step before extending analysis of such a complex trait to multiple species. For example, we now know future research on rattlesnake V2R expression should focus on developing juveniles.

We expanded our prior understanding of the rattlesnake chemosensory architecture (Hogan et al. 2021) with robust genetic accounting and updated sequence analyses afforded by a chromosome-resolution genome assembly for *C. adamanteus* (Hogan et al. 2024). We determined V2R gene expression in the vomeronasal epithelium was almost entirely limited to juvenile snakes, suggesting sensory programming of the rattlesnake VNO relies on high V2R expression during early life development of the vomeronasal structures. Follow up characterizations of V2R turnover rates and receptor proteomics are necessary to confirm these predictions. We did not observe a similar pattern in the olfactory epithelium and instead found subtle expression biases which we considered more indicative of life history rather than development. Age-related expression biases in the olfactory epithelium was comparable to *C. adamanteus* venom glands (Hogan et al. 2024), suggesting that certain age-biased ORs may be expressed in coordination with age-biased venom genes. This molecular evidence for predatory trait integration builds on a substantial body of prior work reporting predatory trait integration from head morphology (Margres et al. 2015; Wray et al. 2015) and venom changes underlain by expression and chromatin modification (Rokyta et al. 2017; Schonour et al. 2020; Hogan et al. 2024). We also confirmed that sex chromosomes are closely tied to life-history bias in rattlesnake chemoperception, including a potential female-based mechanism for linkage disequilibrium identified on chromosome W. It has been speculated that viperids, including rattlesnakes, lack a mechanism to compensate for the reduced gene expression in the heterogametic sex, i.e. no dosage compensation (Vicoso et al. 2013). However, we identified a set of female-biased W-chromosome TFs (Fig. 3), which we believe could provide such a mechanism by regulating chemoreceptor expression on chromosome Z. Based on the intraspecific genetic diversity of chemosensory repertoires observed in other systems such as humans (Olender et al. 2012), allelic, and copy-number variation could also provide a genomic basis for chemosensory differences between individual rattlesnakes. Since our analyses targeted life history biases using RNA-seq reads mapped to the same reference genome, the direct effects of allelic differences remains unexplored. However, some of the within-group noise observed in our expression analyses could very well be attributed to copy-number variation or similar genome-level differences among individuals. For example, the loci coding for OR\_168\_chrM\_Z and OR\_425\_chrM\_Z (Supplementary Fig. S3b) had inconsistent within-group expression in a few individuals.

Our OR and V2R paralog trees present holistic molecular representations of the rattlesnake chemosensory repertoire and provide a valuable guide for future research on these receptors. From the selection results, we found significantly more positive selection in the transmembrane region of ORs and in the extracellular region of V2Rs (Table 1), highlighting these as potential tuning sites for these chemoreceptors. From the expression results, the OR clades labeled 2 and 6 in the figure (Fig. 4) were identified as having an abundance of male-biased expression originating on chromosome Z. These clades provide reduced OR gene sets for further assessment of positively selected sites, which could reveal male-specific structural differences for detecting male-specific chemosensory targets. We also illustrate the utility of the V2R tree by following up with a macroevolutionary analysis of the highly expressed

V2R gene isolated on chromosome 5, and mapped the evolution of key residues onto the predicted 3D protein structure. Unfortunately, there are no reference V2R crystal structures publicly available; therefore, our implications of V2R structure are currently limited to hypothetical predictions based on sequence homology with metabotropic glutamate receptors. Nevertheless, this exercise demonstrates the value of using molecular evidence to single out important genes from the full genetic repertoire (685 V2R genes) for deeper exploration of evolution across macroevolutionary timescales. Prior genomic research in snakes and lizards report a diversity of V2Rs (Lind et al. 2019; Cooper 1997; Perry et al. 2018) but fail to identify confirmed orthologs between sister species, let alone spanning a major vertebrate clade.

From an applied conservation perspective, our findings merit consideration for rattlesnake conservation through ecologically informative insights. Continuing to build off our molecular framework could lead to a deeper understanding of the sensory requirements and limitations of rattlesnake reproduction, offspring dispersal, and diet specificity. Identification of important sensory pathways could also prevent unintentional human encounters by minimizing overlap between man-made infrastructure and the rattlesnake sensory landscape (Rottenborn et al. 2022). Rattlesnakes rely heavily on chemical cues when returning to overwintering den sites (Weldon et al. 1992), so understanding the limitations of their chemoperception and identifying overlap between sensory cues and anthropogenic byproducts may further improve relocation efforts (Rottenborn et al. 2022) and prevent accidental den destruction or the release of chemical pollutants, which interrupt chemoperception. Our results may also elicit new molecular leads for invasive species management, such as the brown treesnake introduced to Guam (Fritts 1988) and pythons introduced to the Florida Everglades (Dorcas et al. 2012). In particular, our identification of sex-biased chemoreceptor expression and sex chromosome influence on selection presents target genes to track across species, which could eventually lead to the development of pheromone-based attractants for invasive snake trapping efforts. These and other snake management targets require a sound genetic foundation based on molecular evidence, and by bridging chromosome-level genomics with specific life-history factors in the rattlesnake model, this study contributes a substantial improvement to our overall genetic understanding of chemical perception in snakes.

## Acknowledgments

We thank Kenneth P. Wray, Timothy J. Colston, Alyssa Hasinger, Emilie Broussard, Laura E. Koffinas, Rachel Saul, Alex Oliver, and Simone Gable for assistance in collecting and processing animals. We thank Amber N. Brown and the FSU Biology Core for reagents and assistance with molecular protocols. We thank Cynthia Vied and the FSU Translation Sciences Core Facility for assistance with sequencing. We thank Jack Facente for animal husbandry training. Funding for this work was provided by the American Genetic Association (EECG research award to M.P.H.), the National Science Foundation (NSF DEB 1638902 to D.R.R., NSF DEB 1638879 and NSF DEB 1822417 to C.L.P. and DEB 1638872 to H.L.G.), and with support from the Clemson University Genomics and Bioinformatics Facility, which receives support from the

College of Science and two Institutional Development Awards (IDeA) from the National Institute of General Medical Sciences of the National Institutes of Health under grant numbers P20GM146584 and P20GM139769.

## Author contributions

Michael P. Hogan (Conceptualization, Data curation, Formal analysis, Funding acquisition, Investigation, Methodology, Project administration, Resources, Validation, Visualization, Writing—original draft, Writing—review & editing), Matthew L. Holding (Data curation, Investigation, Methodology, Resources, Supervision, Validation, Writing—review & editing), Gunnar S. Nystrom (Data curation, Investigation, Resources, Writing—review & editing), Kylie C. Lawrence (Data curation, Investigation, Resources, Writing—review & editing), Emilie M. Broussard (Data curation, Investigation, Resources, Writing—review & editing), Schyler A. Ellsworth (Data curation, Investigation, Resources, Writing—review & editing), Andrew J. Mason (Data curation, Investigation, Methodology, Resources, Validation, Writing—review & editing), Mark J. Margres (Project administration, Validation, Writing—review & editing), H. Lisle Gibbs (Data curation, Funding acquisition, Investigation, Methodology, Project administration, Resources, Supervision, Validation, Writing—review & editing), Christopher L. Parkinson (Data curation, Funding acquisition, Methodology, Project administration, Resources, Validation, Writing—review & editing), and Darin R. Rokyta (Conceptualization, Data curation, Formal analysis, Funding acquisition, Investigation, Methodology, Project administration, Resources, Supervision, Validation, Writing—review & editing)

## Supplementary material

Supplementary material is available at *Journal of Heredity* online.

## Conflict of interest statement

None declared.

## Data availability

The genome assembly for *C. adamanteus* has been deposited at DDBJ/ENA/GenBank under the accessions JAOTJ000000000 and BioProjects PRJNA868880, PRJNA88989, and PRJNA667573. The SRA accession status for all chemosensory RNA-seq samples are listed in [Supplementary Table S3](#), and the vertebrate genome accessions are included in [Supplementary Table S4](#).

## Literature Cited

- Alving WR, Kardong KV. The role of the vomeronasal organ in rattlesnake (*Crotalus viridis oreganus*) predatory behavior. *Brain Behav Evol.* 1996;48:165–172.
- Baldwin M, Ko MC. Functional evolution of vertebrate sensory receptors. *Hormones Behav.* 2020;124:104771.
- Benjamini Y, Hochberg Y. Controlling the false discovery rate: a practical and powerful approach to multiple testing. *J R Stat Soc: Ser B (Methodol).* 1995;57:289–300.
- Bertoni M, Kiefer F, Biasini M, Bordoli L, Schwede T. Modeling protein quaternary structure of homo- and hetero-oligomers beyond binary interactions by homology. *Sci Rep.* 2017;7:10480.

- Chernomor O, von Haeseler A, Minh B. Terrace aware data structure for phylogenomic inference from supermatrices. *Syst Biol.* 2016; 65:997–1008.
- Chess A, Simon I, Cedar H, Axel R. Allelic inactivation regulates olfactory receptor gene expression. *Cell.* 1994;78:823–834.
- Cohanin A, Amsalem E, Saad R, Privman E. Evolution of olfactory functions on the fire ant social chromosome. *Genome Biol Evol.* 2018;10:2947–2960.
- Cooper W. Independent evolution of squamate olfaction and vomerolfaction and correlated evolution of vomerolfaction and lingual structure. *Amphibia-Reptilia.* 1997;18:85–105.
- de March CA, Matsunami H, Abe M, Cobb M, Hoover KC. Genetic and functional odorant receptor variation in the homo lineage. *Iscience.* 2023;26:105908.
- Dong D, He G, Zhang S, Zhang Z. Evolution of olfactory receptor genes in primates dominated by birth-and-death process. *Genome Biol Evol.* 2009;1:258–264.
- Dorcas ME, Willson JD, Reed RN, Snow RW, Rochford MR, Miller MA, Meshaka Jr WE, Andreadis PT, Mazzotti FJ, Romagosa CM, et al. Severe mammal declines coincide with proliferation of invasive Burmese pythons in Everglades National Park. *Proc Natl Acad Sci.* 2012;109:2418–2422.
- Du J, Wang D, Fan H, Xu C, Tai L, Lin S, Han S, Tan Q, Wang X, Xu T, et al. Structures of human mGlu2 and mGlu7 homo- and heterodimers. *Nature.* 2021;594:589–593.
- Duvall D, Arnold SJ, Schuett GW. Pitviper mating systems: ecological potential, sexual selection, and microevolution. In: Campbell JA, Brodie ED, editors. *Biology of the Pitvipers*. Tyler (TX): Selva Publishing; 1992. p. 321–336. ISBN 978-0963053701.
- Fritts TH. *The brown tree snake, Boiga irregularis, a threat to Pacific islands*, vol. 88. US Department of the Interior, Fish and Wildlife Service, Research and Development. 1988.
- Giorgianni M, Dowell N, Griffin S, Kassner V, Selegue J, Carroll S. The origin and diversification of a novel protein family in venomous snakes. *Proc Natl Acad Sci.* 2020;117:201920011.
- Gracheva E, Ingolia N, Kelly Y, Cordero-Morales J, Holoopeter G, Chesler A, Sánchez E, Pérez J, Weissman J, Julius D. Molecular basis of infrared detection by snakes. *Nature.* 2010;464: 1006–1011.
- Guex N, Peitsch M, Schwede T. Automated comparative protein structure modeling with SWISS-MODEL and Swiss-PdbViewer: a historical perspective. *Electrophoresis.* 2009;30:S162–S173.
- Guindon S, Dufayard JF, Lefort V, Anisimova M, Hordijk W, Gascuel O. New algorithms and methods to estimate maximum-likelihood phylogenies: assessing the performance of PhyML 3.0. *Syst Biol.* 2010;59:307–321.
- Hansson BS, Stensmyr MC. Evolution of insect olfaction. *Neuron.* 2011;72:698–711.
- Hoang D, Chernomor O, von Haeseler A, Minh B, Vinh L. UFBoot2: improving the ultrafast bootstrap approximation. *Mol Biol Evol.* 2017;35:518–522.
- Hogan MP, Holding ML, Nystrom GS, Colston TJ, Bartlett DA, Mason AJ, Ellsworth SA, Rautsaw RM, Lawrence KC, Strickland JL, et al. The genetic regulatory architecture and epigenomic basis for age-related changes in rattlesnake venom. *Proc Natl Acad Sci.* 2024; 121:e2313440121.
- Hogan MP, Whittington AC, Broe MB, Ward MJ, Gibbs HL, Rokyta DR. The chemosensory repertoire of the eastern diamondback rattlesnake (*Crotalus adamanteus*) reveals complementary genetics of olfactory and vomeronasal-type receptors. *J Mol Evol.* 2021; 89:313–328.
- Holding ML, Strickland JL, Rautsaw RM, Hofmann EP, Mason AJ, Hogan MP, Nystrom GS, Ellsworth SA, Colston TJ, Borja M, et al. Phylogenetically diverse diets favor more complex venoms in North American pitvipers. *Proc Natl Acad Sci.* 2021;118:e2015579118.
- Hughes G, Boston E, Finarelli J, Murphy W, Higgins D, Teeling E. The birth and death of olfactory receptor gene families in mammalian niche adaptation. *Mol Biol Evol.* 2018;35: 1390–406.

- Kalyaanamoorthy S, Minh B, Wong T, von Haeseler A, Jermini L. ModelFinder: fast model selection for accurate phylogenetic estimates. *Nat Methods*. 2017;14:587–591.
- Kardong KV, Berkhoudt H. Rattlesnake hunting behavior: correlations between plasticity of predatory performance and neuroanatomy. *Brain Behav Evol*. 1999;53:20–28.
- Kawajiri M, Yoshida K, Fujimoto S, Mokodongan DF, Ravinet M, Kirkpatrick M, Yamahira K, Kitano J. Ontogenetic stage-specific quantitative trait loci contribute to divergence in developmental trajectories of sexually dimorphic fins between Medaka populations. *Mol Ecol*. 2014;23:5258–5275.
- Khan I, Yang Z, Maldonado E, Li C, Zhang G, Gilbert M. Olfactory receptor subgenomes linked with broad ecological adaptations in sauropsids. *Mol Biol Evol*. 2015;32:2832–2843.
- Kim D, Paggi JM, Park C, Bennett C, Salzberg SL. Graph-based genome alignment and genotyping with HISAT2 and HISAT-genotype. *Nat Biotechnol*. 2019;37:907–915.
- Kishida T, Go Y, Tatsumoto S, Tatsumi K, Kuraku S, Toda M. Loss of olfaction in sea snakes provides new perspectives on the aquatic adaptation of amniotes. *Philos Trans R Soc Lond B*. 2019;286:20191828.
- Kishida T, Hikida T. Degeneration patterns of the olfactory receptor genes in sea snakes. *J Evol Biol*. 2010;23:302–310.
- Kishida T, Kubota S, Shirayama Y, Fukami H. The olfactory receptor gene repertoires in secondary-adapted marine vertebrates: evidence for reduction of the functional proportions in cetaceans. *Biol Lett*. 2007;3:428–430.
- Leticia I, Bork P. Interactive Tree Of Life (iTOL) v4: recent updates and new developments. *Nucleic Acids Res*. 2019;47:W256–W259.
- Li H, Handsaker B, Wysoker A, Fennell T, Ruan J, Homer N, Marth G, Abecasis G, Durbin R, 1000 Genome Project Data Processing Subgroup. The sequence alignment/map format and SAMtools. *Bioinformatics*. 2009;25:2078–2079.
- Lind A, Lai Y, Mostovoy Y, K Holloway A, Iannucci A, CY Mak A, Fondi M, Orlandini V, Eckalbar W, Milan M, et al. A high-resolution, chromosome-assigned Komodo dragon genome reveals adaptations in the cardiovascular, muscular, and chemosensory systems of monitor lizards. *Nat Ecol Evol*. 2019;3:1241–1252.
- Liu A, He F, Shen L, Liu R, Wang Z, Zhou J. Convergent degeneration of olfactory receptor gene repertoires in marine mammals. *BMC Genomics*. 2019;20.
- Love MI, Huber W, Anders S. Moderated estimation of fold change and dispersion for RNA-seq data with DESeq2. *Genome Biol*. 2014;15:550.
- Lu S, Wang J, Chitsaz F, Derbyshire M, Geer R, Gonzales N, Gwadz M, Hurwitz D, Marchler G, Song J, et al. CDD/SPARCLE: the conserved domain database in 2020. *Nucleic Acids Res*. 2019;48:1–4.
- Marchler-Bauer A, Derbyshire M, Gonzales N, Lu S, Chitsaz F, Geer L, Geer R, He J, Gwadz M, Hurwitz D, et al. CDD: NCBI's conserved domain database. *Nucleic Acids Res*. 2014;43:D222–D226.
- Margres MJ, Walls R, Suntrav M, Lucena S, Sánchez EE, Rokyta DR. Functional characterizations of venom phenotypes in the eastern diamondback rattlesnake (*Crotalus adamanteus*) and evidence for expression-driven divergence in toxic activities among populations. *Toxicon*. 2016;119:28–38.
- Margres MJ, Wray KP, Seavy M, McGivern JJ, Sanader D, Rokyta DR. Phenotypic integration in the feeding system of the eastern diamondback rattlesnake (*Crotalus adamanteus*). *Mol Ecol*. 2015;24:3405–3420.
- Mason AJ, Holding ML, Rautsaw RM, Rokyta DR, Parkinson CL, Gibbs HL. Venom gene sequence diversity and expression jointly shape diet adaptation in pitvipers. *Mol Biol Evol*. 2022;39:msac082.
- Means DB. Food and prey acquisition. In: *Diamonds in the rough: natural history of the eastern diamondback rattlesnake*. Tallahassee (FL): Tall Timbers Press. ISBN 978-0-9703886-5-0; 2017. p. 173–198.
- Mombaerts P. Genes and ligands for odorant, vomeronasal and taste receptors. *Nat Rev Neurosci*. 2004;5:263–278.
- Murrell B, Wertheim J, Moola S, Weighill T, Scheffler K, Pond S. Detecting individual sites subject to episodic diversifying selection. *PLoS Genet*. 2012;8:e1002764.
- Nei M, Rooney AP. Concerted and birth-and-death evolution of multigene families. *Annu Rev Genet*. 2005;39:121–152.
- Nguyen LT, Schmidt H, von Haeseler A, Minh B. IQ-TREE: a fast and effective stochastic algorithm for estimating maximum-likelihood phylogenies. *Mol Biol Evol*. 2014;32:268–274.
- Niimura Y. On the origin and evolution of vertebrate olfactory receptor genes: comparative genome analysis among 23 chordate species. *Genome Biol Evol*. 2009;1:34–44.
- Niimura Y, Nei M. Evolutionary dynamics of olfactory and other chemosensory receptor genes in vertebrates. *J Hum Genet*. 2006;51:505–517.
- Niimura Y, Nei M. Extensive gains and losses of olfactory receptor genes in mammalian evolution. *PLoS One*. 2007;2:e708.
- Olender T, Waszak SM, Viavant M, Khen M, Ben-Asher E, Reyes A, Nativ N, Wysocki CJ, Ge D, Lancet D. Personal receptor repertoires: olfaction as a model. *BMC Genomics*. 2012;13:1–16.
- Paradis E, Schliep K. ape 5.0: an environment for modern phylogenetics and evolutionary analyses in R. *Bioinformatics*. 2019;35:526–528.
- Peng ZL, Wu W, Tang CY, Ren JL, Jiang D, Li JT. Transcriptome analysis reveals olfactory system expression characteristics of aquatic snakes. *Front Genet*. 2022;13:34.
- Perry B, Card D, McGlothlin J, Pasquesi G, Adams R, Schield D, Hales N, Corbin A, P Demuth J, Hoffmann F, et al. Molecular adaptations for sensing and securing prey and insight into amniote genome diversity from the garter snake genome. *Genome Biol Evol*. 2018;10:2110–2129.
- Pond S, Frost S. Not so different after all: a comparison of methods for detecting amino acid sites under selection. *Mol Biol Evol*. 2005;22:1208–1222.
- Pond S, Poon A, Velazquez R, Weaver S, Hepler N, Murrell B, Shank S, Rife Magalis B, Bouvier D, Nekrutenko A, et al. Hyphy 2.5—a customizable platform for evolutionary hypothesis testing using phylogenies. *Mol Biol Evol*. 2019;37:295–299.
- Putri GH, Anders S, Pyl PT, Pimanda JE, Zanini F. Analysing high-throughput sequencing data in python with HTSeq 2.0. *Bioinformatics*. 2022;38:2943–2945.
- Rokyta DR, Lemmon AR, Margres MJ, Aronow K. The venom-gland transcriptome of the eastern diamondback rattlesnake (*Crotalus adamanteus*). *BMC Genomics*. 2012;13:312.
- Rokyta DR, Margres MJ, Ward MJ, Sanchez EE. The genetics of venom ontogeny in the eastern diamondback rattlesnake (*Crotalus adamanteus*). *Peer J*. 2017;5:e3249.
- Rosenbaum D, Rasmussen S, Kobilka B. The structure and function of G-protein-coupled receptors. *Nature*. 2009;459:356–63.
- Rottenborn M, Bedard R, Taylor E. *Mitigation translocation as a management strategy for human-snake conflict in California*. Technical report, California Department of Fish and Wildlife. 2022.
- Saviola AJ, Chiszar D, Busch C, Mackessy SP. Molecular basis for prey relocation in viperid snakes. *BMC Biol*. 2013;11:20.
- Sayers EW, Bolton EE, Brister JR, Canese K, Chan J, Comeau DC, Connor R, Funk K, Kelly C, Kim S, et al. Database resources of the national center for biotechnology information. *Nucleic Acids Res*. 2022;50:D20–D26.
- Schild D, Card D, Hales N, Perry B, Pasquesi G, Blackmon H, Adams R, Corbin A, Smith C, Ramesh B, et al. The origins and evolution of chromosomes, dosage compensation, and mechanisms underlying venom regulation in snakes. *Genome Res*. 2019;29:590–601.
- Schonour RB, Huff EM, Holding ML, Claunch NM, Ellsworth SA, Hogan MP, Wray K, McGivern J, Margres MJ, Colston TJ, et al. Gradual and discrete ontogenetic shifts in rattlesnake venom composition and assessment of hormonal and ecological correlates. *Toxins*. 2020;12:659.
- Shannon P, Markiel A, Ozier O, Baliga NS, Wang JT, Ramage D, Amin N, Schwikowski B, Ideker T. Cytoscape: a software environment for

- integrated models of biomolecular interaction networks. *Genome Res.* 2003;13:2498–2504.
- Sievers F, Wilm A, Dineen D, Gibson TJ, Karplus K, Li W, Lopez R, McWilliam H, Remmert M, Söding J, et al. Fast, scalable generation of high-quality protein multiple sequence alignments using Clustal Omega. *Mol Syst Biol.* 2011;7:539.
- Simoes BF, Foley NM, Hughes GM, Zhao H, Zhang S, Rossiter SJ, Teeling EC. As blind as a bat? Opsin phylogenetics illuminates the evolution of color vision in bats. *Mol Biol Evol.* 2018;36:54–68.
- Stranger BE, Forrest MS, Dunning M, Ingle CE, Beazley C, Thorne N, Redon R, Bird CP, de Grassi A, Lee C, et al. Relative impact of nucleotide and copy number variation on gene expression phenotypes. *Science.* 2007;315:848–853.
- UniProt Consortium. UniProt: a hub for protein information. *Nucleic Acids Res.* 2015;43:D204–D212.
- Vicoso B, Emerson J, Zektser Y, Mahajan S, Bachtrog D. Comparative sex chromosome genomics in snakes: differentiation, evolutionary strata, and lack of global dosage compensation. *PLOS Biol.* 2013;11:1001643.
- Waterhouse A, Bertoni M, Bienert S, Studer G, Tauriello G, Gumienny R, T Heer F, A P de Beer T, Rempfer C, Bordoli L, et al. SWISS-MODEL: homology modelling of protein structures and complexes. *Nucleic Acids Res.* 2018;46:W296–W303.
- Weldon PJ, Ortiz R, Sharp TR. The chemical ecology in crotaline snakes. In: Campbell JA, Brodie ED, editors. *Biology of the pitvipers*. Tyler (TX): Selva Publishing. ISBN 978-0963053701; 1992. p. 309–319.
- Wray KP, Margres MJ, Seavy M, Rokyta DR. Early significant ontogenetic changes in snake venoms. *Toxicon.* 2015;96:74–81.
- Wu H, Wang C, Gregory K, Han G, Cho H, Xia Y, Niswender C, Katritch V, Meiler J, Cherezov V, et al. Structure of a class C GPCR metabotropic glutamate receptor 1 bound to an allosteric modulator. *Science.* 2014;344:58–64.